Preprint Title **Theranostic polymeric nanocarriers modified by enhanced gadolinium conjugation techniques**

Authors Tivadar Feczkó, Albrecht Piiper, Thomas Pleli, Christian Schmithals, Dominic Denk, Thomas J. Vogl and Matthias G. Wacker

Article Type Full Research Paper

ORCID® iDs Tivadar Feczkó - https://orcid.org/0000-0002-6119-7922; Dominic Denk - https://orcid.org/0000-0002-4887-1492; Matthias G. Wacker - https://orcid.org/0000-0002-2789-6463

Theranostic polymeric nanocarriers modified by enhanced gadolinium conjugation techniques

Tivadar Feczkó[1,2*], Albrecht Piiper[3], Thomas Pleli[3], Christian Schmithals[3], Dominic Denk[3] Thomas J. Vogl[4], Matthias G. Wacker[5]

[1] Research Centre for Natural Sciences, Hungarian Academy of Sciences, Magyar tudosok krt. 2., Budapest H-1117, Hungary
[2] Research Institute of Biomolecular and Chemical Engineering, University of Pannonia, Egyetem u. 2., Veszprém H-8200, Hungary
[3] Department of Medicine 1, University Hospital Frankfurt, Theodor-Stern-Kai 7, Frankfurt D-60590, Germany
[4] Department of Diagnostic and Interventional Radiology, University Hospital Frankfurt, Theodor-Stern-Kai 7, Frankfurt D-60590, Germany
[5] Department of Pharmacy, National University of Singapore, 6 Science Drive 2, Singapore 117559, Singapore

Email: Tivadar Feczkó - feczko@mukki.richem.hu

* Corresponding author

1. Abstract

Background: Efficient delivery of the poorly water-soluble compound sorafenib still poses a challenge to current formulation strategies. To incorporate the lipophilic molecule into biocompatible and biodegradable theranostic nanoparticles has great potential for improving efficacy and safety of cancer therapy.

Results: In this study, sorafenib nanoencapsulation was optimized using poly(D,L-lactide-co-glycolide) and polyethylene glycol-poly(D,L-lactide-co-glycolide) copolymers comparing three different technologies. The particles ranged in size between 220 and 240 nm with encapsulation efficiencies from 76.1 ± 1.7 % to 69.1 ± 10.1 %. A remarkable maximum drug load of 9.0 % was achieved. Finally, a gadolinium complex was covalently attached to the nanoparticle surface transforming the nanospheres into theranostic devices allowing the localization using magnetic resonance imaging.

Conclusion: The manufacture of sorafenib-loaded nanoparticles and the functionalization of the particle surface with a gadolinium complex resulted in a high drug loading, a strong MRI signal, optimal stability features and a sustained release profile.

2. Keywords

gadolinium; drug release; polymeric nanocarrier; sorafenib; theranostic nanoparticles

3. Introduction

Hepatocellular carcinoma (HCC) is a life-threatening disease and, according to global cancer statistics from 2012, the third leading cause of cancer-related deaths in men and the sixth in women, worldwide [1]. At present, sorafenib is the only drug available prolonging the life of patients with HCC. However, the non-specific uptake of the drug into healthy tissues leads to a high toxicity and a variety of serious adverse reactions [2].

Sorafenib is a multi-kinase inhibitor targeting various receptor tyrosine kinases and rapidly accelerated fibrosarcoma (RAF) kinases. Hence, it reduces tumour growth leading to significantly improved survival rates [1, 2]. However, a pronounced lipophilicity of the molecule is responsible for the poor bioavailability and distribution of the compound into healthy tissues [2, 3]. As a consequence, drug therapy is accompanied by serious side effects and a high dose is required.

Against this background, nanocarrier-based delivery of sorafenib has the potential to improve drug therapy significantly. Theranostic nanodelivery systems offer a versatile combination of therapeutic and diagnostic features and have been applied to this task earlier [3, 4]. A variety of contrast agents such as gadolinium diethylenetriamine pentaacetic acid (Gd-DTPA), shorten the longitudinal relaxation time, and were widely used for both vascular and tumor magnetic resonance imaging (MRI) [4, 5]. One major limitation of this technique lies in the short half-life of the contrast agent as well as the poor specificity for the target site.

In this context, Gd-DTPA-conjugated human serum albumin (HSA) nanoparticles improved the contrast of MRI compared to Gd-DTPA aqueous solution *in vivo* [3-5]. Unfortunately, even after conjugation of polyethylene glycol (PEG) to the particle surface, HSA

nanoparticles exhibit only short circulation time [6] and the potential for scale-up of this technology is rather limited [7].

On the contrary, block copolymers comprising polylactic-co-glycolic acid (PLGA) and PEG were processed to nanoparticles at medium-scale using microfluidic technology [8] and emulsion techniques [9]. Recently, formulations manufactured by BIND Therapeutics successfully passed phase 1 clinical trials [10]. A major shortcoming of nanocarrier delivery can be the limited drug load resulting in a high excipient concentrations and administration volume [11]. Previous investigations reported the loading of sorafenib into PLGA nanoparticles achieving a drug load of 1.4% [12]. An oil-in-water single emulsion-solvent evaporation method was used. Preparations made with a nanoprecipitation-dialysis technique using a block copolymer comprising dextran and PLGA resulted in a drug load of 5.3% [13]. To attain synergistic effects of cytostatic agents, co-delivery of drug molecules has been approached. By employing a novel sequential freeze-thaw method followed by ethanol coacervation, a core-shell construct was manufactured [14]. After preparation of a polyvinyl alcohol (PVA)-doxorubicin nanocore, a thin shell of HSA comprises sorafenib as a second drug molecule. A drug load of 2.4 % was reached. Lipid-polymer hybrid nanoparticles were synthesized for the co-delivery of doxorubicin and sorafenib to enhance efficacy in HCC therapy [15].

Other approaches focused on theranostic drug delivery systems containing gadolinium (Gd) and sorafenib. Theranostic liposomal carriers with a drug content of 4.3 % [m/m] were produced [16]. Another system used a multiblock polymer comprising (poly(lactic acid)-poly(ethylene glycol)-poly(L-lysine)-diethylenetriamine pentaacetic acid and the pH-sensitive material poly(L-histidine)-poly(ethylene glycol)-biotin. A drug content of 2.4 % [m/m] of

sorafenib was reached and the MRI signal intensity was more beneficial than the one of Magnevist® *in vivo* [12].

In the present study, the impact of three different techniques for the nanoencapsulation of sorafenib into PLGA and polyethylene glycol-poly(D,L-lactide-co-glycolide) copolymer (PEG-PLGA) nanocarriers have been compared and the effect of the encapsulation method on drug load and other physicochemical properties has been studied. Among the methods evaluated, namely nanoprecipitation, single and double emulsion-solvent evaporation, the single emulsion-solvent evaporation was found to result in the optimal product parameters, thus, this process was optimized with regards to the intended target product profile. *In vitro* cytotoxicity and cellular uptake were investigated in HepG2 cells. Finally, the nanoparticles were modified on their surface using a Gd complex resulting in a theranostic nanocarrier system. For this purpose, the encapsulation of HSA into nanoparticles as well as the covalent modification of the surface using HSA or polyethylene imine were approached.

4. Results and discussion

In recent years, a variety of preparation methods have been evaluated for the synthesis of nanocarrier devices. The current approach resulted in advanced theranostic drug carriers and compared the impact of manufacturing technology and surface modification on the physicochemical properties and *in vitro* features. Initially, a particle size between 100 and 300 nm [17], a zeta potential of more than -15 mV [18, 19], a high drug load and particle yield were identified as key criteria for formulation development. Among other aspects, the encapsulation efficiency and particle size play an important role in nanocarrier delivery.

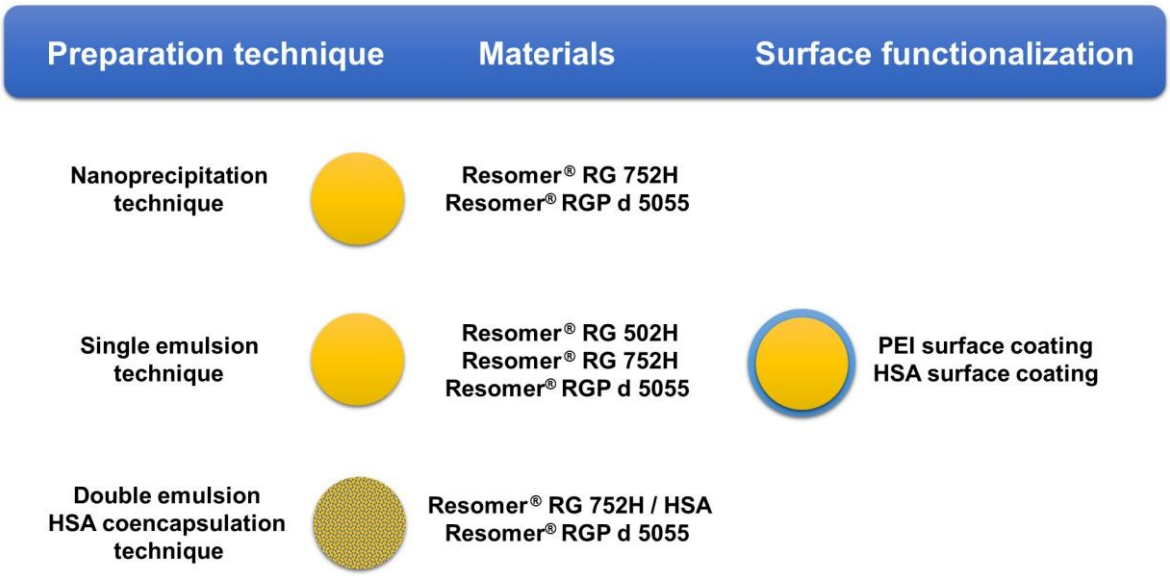

Figure 1: Scheme of the nanoparticle preparations with the preparation technique, materials used and surface functionalization (from the left to the right).

Selecting biodegradable polymers from the Resomer® family, three different techniques for the encapsulation of sorafenib were compared (Figure 1).

a. Manufacture of sorafenib-loaded Resomer® core particles using nanoprecipitation and single emulsion technique

As a first technique, nanoprecipitation with Triton X-100 and Pluronic F127 as stabilizing agents resulted in a pronounced aggregation of the nanoparticles for all polymers. Similar observations have been made in medium-scale suggesting also a poor 'scalability' during later stages of process translation [8].

When using a combination of Resomer® RG 502H or Resomer® RGP d 5055 and PVA as a stabilizer, a particle system broadly distributed in size was indicated by the elevated PDI values between 0.27 and 0.46. This was also confirmed by the intensity distribution showing a second and third fraction of larger particles in the micro range (Figure 2).

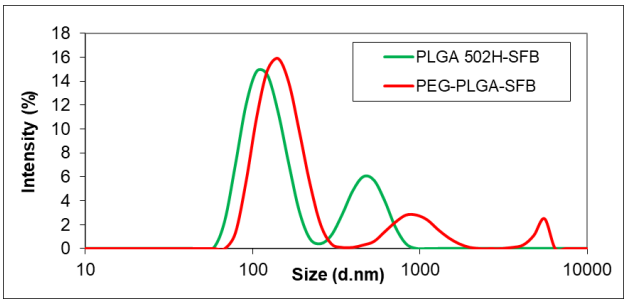

Figure 2: Size distribution by intensity of nanocomposites containing sorafenib in a Resomer® RG 502H PLGA (PLGA 502H-SFB) and Resomer® RGP d 5055 PEG-PLGA (PEG-PLGA-SFB) matrix nanoparticles prepared by nanoprecipitation using PVA as an emulsifier.

The formation of drug crystals of sorafenib was assumed. Similar PDI values (0.21-0.35) were reported by [18] using the nanoprecipitation technique. Exclusively, a particle size in the desired range (196 ± 10 nm) and reduced PDI values (0.21 ± 0.03) were achieved when using Resomer® RG 752H PLGA polymer (Figure 3).

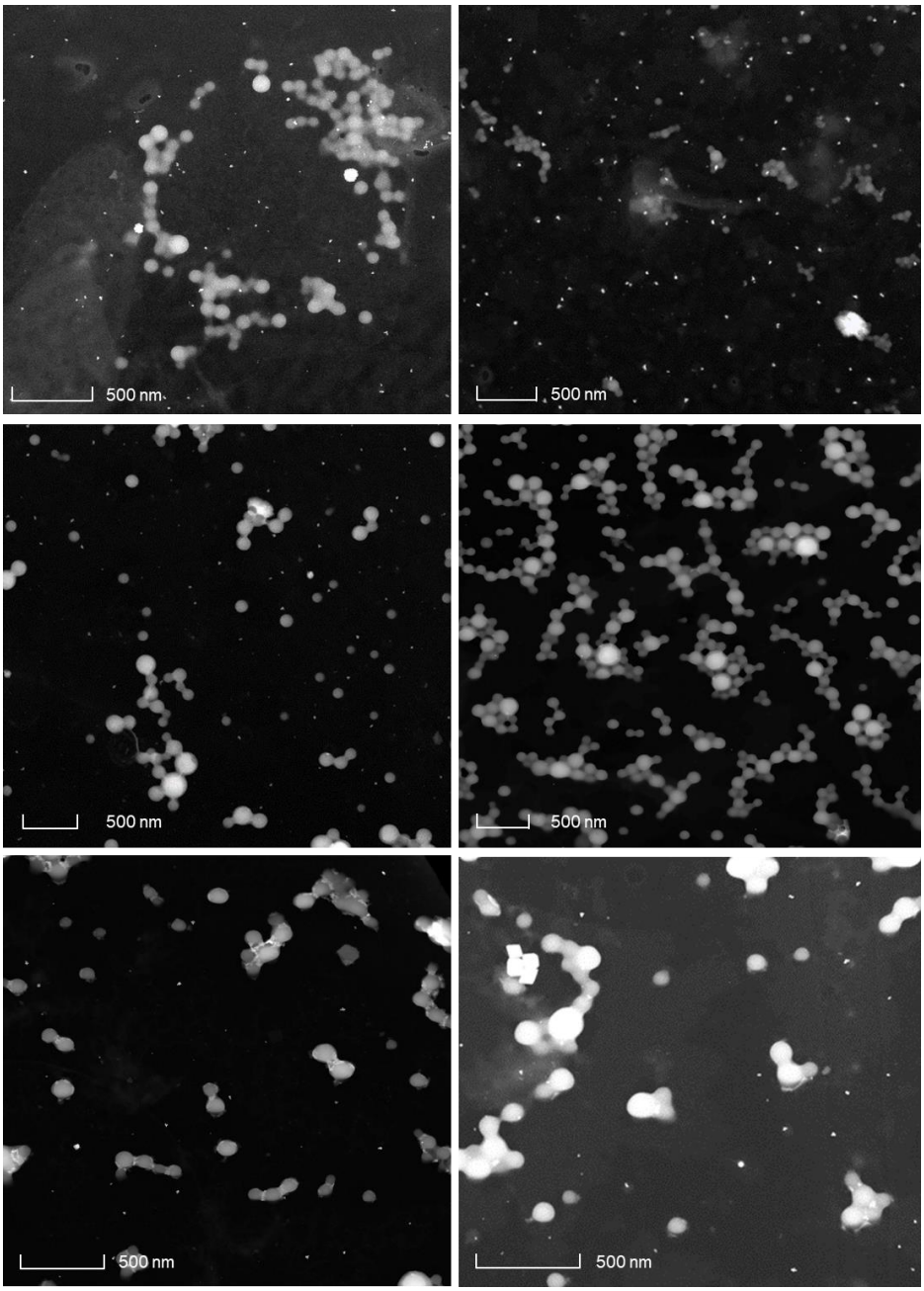

Figure 3: S/TEM image of nanoparticles comprising sorafenib in a Resomer® RG 752H PLGA (upper left) matrix and Resomer® RGP d 5055 (upper right) prepared by nanoprecipitation. Scanning/transmission electron micrographs of Resomer RG 752H PLGA-sorafenib (middle left) and Resomer®, RGP d 5055-sorafenib (middle right) nanocomposites prepared by double emulsion technique and Resomer RG 752H PLGA-sorafenib (lower left) and Resomer®, RGP d 5055-sorafenib (lower right) nanocomposites prepared by single emulsion-solvent evaporation.

This aggregation also occurred using a combination of Resomer® RG 502H or Resomer® RG 752H and Tween® 80 surfactant for the nanoprecipitation of the nanocomposites. Differently, Resomer® RGP d 5055 nanoparticles were in the desirable size range (153 ± 14 nm) with the same technology (Figure 3), but exhibited a high PDI value (>0.27), poor encapsulation

efficiency (<20 %) and particle yield (20-40 %). A lower density of the particle system due to the hydrophilic side chains of the polymer is the most likely explanation. Considering the difficulties in nanoparticle preparation when using the nanoprecipitation method, later efforts were focused on nanoparticle manufacture by single and double emulsion techniques. PVA turned out to be the optimal stabilizing agent resulting in monomodal size distribution of the nanospheres (Figure 4), an increased drug load (10 % (m/m)) and parameters within the specified range for each of the three polymers (Table 1).

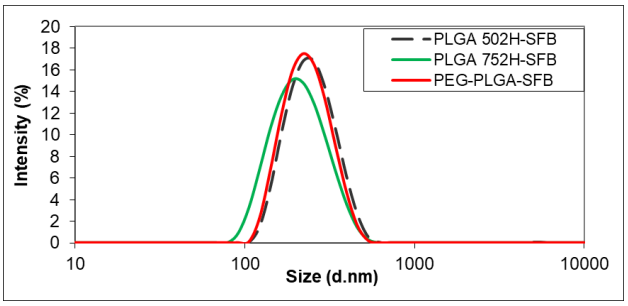

Figure 4: Size distribution by intensity of sorafenib containing nanoparticles prepared from Resomer® RG 502H (PLGA 502H-SFB) and Resomer® RG 752H (PLGA 752H-SFB) PLGA polymers as well as Resomer® RGP d 5055 PEG-PLGA copolymer (PEG-PLGA-sorafenib) by emulsion-solvent evaporation method.

Table 1: Properties of (PEG-)PLGA-sorafenib nanoparticles as a function of encapsulating polymer and emulsifier (PVA) concentration.

	PLGA (RG 502H)	PLGA RG 752H)	PEG-PLGA (d5055)	PLGA (RG 502H)	PLGA (RG 752H)	PEG-PLGA (RGP d5055)
PVA (% w/v)	1	1	1	2	2	2
Mean size by intensity (nm)	235	227.7	228.3	231.4	231.3	243.4
PDI	0.14	0.18	0.12	0.15	0.19	0.15
Zeta potential (mV)	-21.3	-22.4	-19.7	-19.8	-22.2	-19.5
Encapsulation efficiency (%)	70.4	76.2	76.7	76.5	78.8	74.9
Yield (%)	78.3	74.4	76.8	70.2	72.0	76.8

A concentration of 10 mg/ml of the polymer (in DCM), an initial drug concentration of 10 % (m/m) and a water-to-oil ratio of 4:1 resulted in the particle properties presented in Table 1. Further increase of the drug amount from 10 % to 20 % resulted in elevated PDI values (Table

2) denoting the presence of larger aggregates formed during the preparation process. For optimized condition with 10 mg/ml encapsulating polymer concentration and 10 % initial drug ratio, using Resomer® RG 752H PLGA, a nanoparticle yield of 73.7 ± 4.1 % and an encapsulation efficiency of 69.1 ± 10.1 %, have been achieved. Interestingly, the entrapment under the same condition into the Resomer® RGP d 5055 polymer resulted in even higher particle yield of 76.1 ± 1.7 % with an encapsulation efficiency of 75.2 ± 1.2 %. An average drug load of 8.53 % for Resomer® RG 752H PLGA-sorafenib and 8.99 % for Resomer® RGP d 5055 was calculated. Zeta potential values varied between -22.4 mV and – 19.5 mV indicating stability of the colloid system.

Table 2: Mean size (nm) and PDI of (PEG-)PLGA-sorafenib nanoparticles as a function of used ratio of sorafenib (m/m % related to the polymer mass).

	PLGA (RG 752H)			PEG-PLGA (RGP d 5055)		
Sorafenib initial ratio (m/m %)	40	20	10	40	20	10
Mean size by intensity (nm)	242.8	219.3	222.4	287.8	243.7	230.5
PDI	0.40	0.33	0.12	0.46	0.35	0.12

In summary, the top-down approach using the emulsion technique turned out to be more robust compared to the nanoprecipitation method. The nanoparticles were in the size range and exhibited optimal properties for further processing.

b. Modification of the particle matrix using HSA co-encapsulation or surface coating techniques

To covalently bind the Gd complex to the particle surface, amino groups were introduced into the polymeric matrix. In a first approach, HSA was co-encapsulated into the nanoparticles using the double emulsion-solvent evaporation method. The HSA incorporation resulted in smaller particle size than with single emulsion method, although there was no significant

difference between the diameters of nanoparticles formed using PLGA and PEG-PLGA polymers (mean size by intensity: 210.6 nm and 210.3 nm, PDI: 0.099 and 0.113 for Resomer RG 752H PLGA-sorafenib and Resomer®, RGP d 5055 PEG-PLGA-sorafenib, respectively. The morphology of the nanocomposites was similarly spherical by double emulsion (Figure 3, middle) as with nanoprecipitation (Figure 3, upper) and single emulsion methods (Figure 3, lower).

The particle yield of the resulting nanocomposites was much lower compared to the methods described earlier. A particle yield of 50.4 ± 1.0 % for Resomer® RG 752H and 49.0 ± 5.3 % for Resomer® RGP d 5055 was achieved. Similar amount of HSA was incorporated by the PLGA and PEG-PLGA polymers (Resomer® RG 752H 10.6 %, Resomer® RGP d 5055, 9.4 %). The formation of smaller particles with reduced density can be responsible for the decreased particle yield. However, the incorporation method resulted in a high protein loading and an increased number of functional groups available for the EDC reaction. In comparison, an amount of 1.0 ± 0.3 % HSA for Resomer® RG 752H and 1.9 ± 0.5 % HSA for Resomer® RGP d 5055, was bound to the particles using the surface coating technique.

c. Surface modification with gadolinium

Gd-DTPA was conjugated to the amino groups of the HSA molecules after incorporation or covalent binding of the protein to PLGA and PEG-PLGA nanoparticles. As expected, the modification of nanocomposites with gadolinium was limited by the availability of functional groups on the particle surface. Nanoparticles modified with HSA on their surface were characterized by a poor binding (PLGA: 1.5 mg Gd/g nanoparticle, PEG-PLGA: 1.4 mg Gd/g nanoparticle). Nanoparticles comprising HSA as part of their matrix structure exhibited a higher binding (PLGA 2.3 mg Gd/g nanoparticle, PEG-PLGA 3.2 mg Gd/g nanoparticle). Nevertheless, further increase of the Gd content was achieved using a method described earlier [20] with some modification (see in 2.9.). Binding PEI to the surface of nanoparticles a

significant increase in the Gd content was achieved (PLGA: 15.7 mg Gd/g nanoparticle, PEG-PLGA: 10.7 mg Gd/g nanoparticle).

d. Evaluation of contrast signal using in vitro MRI

The MRI properties of theranostic nanocarriers were investigated *in vitro*. Magnevist® aqueous solutions containing different concentrations were used as a reference. There was a linear correlation (Figure 5) between the MRI signal and the Gd content in a range between 0.02 and 0.3 mg Gd/ml (with MRI intensities of 470-670 for 0.02 mg Gd/ml, and 1520-1750 for 0.3 mg Gd/ml). For nanoparticles exhibiting the highest content of Gd the theoretical particle concentration (calculated from a maximum injectable particle concentration of 10 mg/ml and the obtained Gd loading) fell into this calibration range. The signal intensities measured for the T1-weighed MRI were in good accordance with the ICP results. Earlier studies reported 4.7-8.5 mg Gd/g nanoparticle concentration in HSA nanoparticles after covalent linking of DTPA to the protein nanoparticles obtained by desolvation, which was found to be considerably high for *in vivo* MRI studies [5].

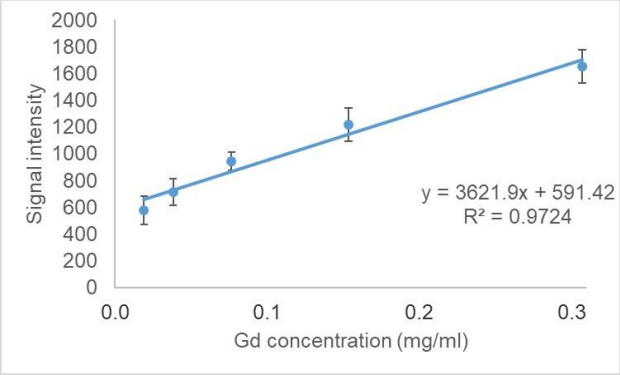

Figure 5: MRI signal intensity as a function of Gd concentration (mg/ml).

e. Storage stability of theranostic nanocomposite formulations

For PLGA particles a concentration of 3 % (w/v) lyoprotector has been used earlier [21]. The sorafenib loaded nanoparticles with a drug load of approximately 10 % were freeze dried in

the presence of 3 % (w/v) trehalose or mannitol. Both PLGA-sorafenib and PEG-PLGA-sorafenib nanospheres remained stable during the time of storage. An increase in the PDI values was observed for formulations freeze-dried with mannitol (Table 3). On this background, trehalose at a concentration of 3 % was identified to be the optimal lyoprotector for the developed particle system (Figure 6).

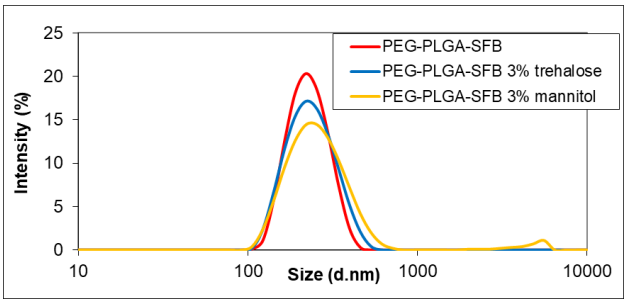

Figure 6: Size distribution by intensity of sorafenib containing Resomer® RGP d 5055 PEG-PLGA nanoparticles after preparation (PEG-PLGA-sorafenib), and following reconstitution after freeze drying in the presence of trehalose (PEG-PLGA-sorafenib 3 % trehalose) and mannitol lyoprotectors (PEG-PLGA-sorafenib 3 % mannitol).

Table 3: Mean size (nm) and PDI of (PEG-)PLGA-sorafenib nanoparticles before and after lyophilisation using trehalose or mannitol lyoprotector.

		before lyophilization	3 % trehalose	3 % mannitol
PLGA (RG 752H)-sorafenib	Size (nm)	229.4	241.8	270.4
	PDI	0.19	0.22	0.28
PEG-PLGA (RGP d 5055)-sorafenib	Size (nm)	217.3	222.2	249.9
	PDI	0.08	0.11	0.21

f. Evaluation of in vitro drug release of sorafenib from theranostic nanocomposites

For nanoparticles comprising polymers from the Resomer® family, a biphasic release pattern has been reported earlier [22]. Preliminary investigations highlighted a less pronounced burst effect for Resomer® RG 752H PLGA compared to Resomer® RG 502H PLGA. After the

initial release phase, a sustained release behaviour has been observed. Consequently, the drug release of PEG-PLGA and PLGA particles was investigated over a time period of 12 days in human blood plasma. The initial burst release was higher with nanoparticles incorporated in Resomer® RG 752H PLGA polymer (18.2 ± 2.9 %). For PEG-PLGA, 8.8 ± 2.1 % of the drug was released during the first hours. Afterwards, a continuous release was observed for both composites (Figure 7). Surprisingly, the release of PEG-PLGA was substantially slower, reaching a plateau at 50.6 ± 9.2 %. A specific interaction with the hydrophilic side chain could be responsible for this behaviour.

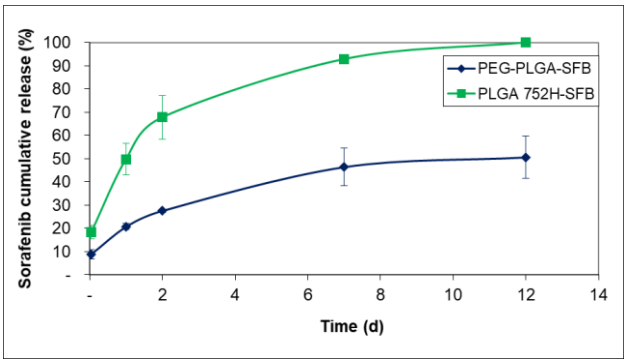

Figure 7: Sorafenib release from Resomer® RG 752H PLGA-sorafenib (PLGA 752H-SFB) and PEG-PLGA-sorafenib (PEG-PLGA-SFB) nanocomposites in human blood plasma. Data are presented as mean ± SD from 3 independent samples for each concentration.

*g. Cellular uptak*e and cytotoxicity

The internalization rates of sorafenib containing nanoparticles in HepG2 cells were determined by flow cytometry. As expected, drug-loaded nanoparticles prepared using the pegylated polymer were taken up by significantly fewer cells (9.6 ± 3.3 %) than Resomer® RG 752H PLGA-sorafenib nanoparticles (25.7 ± 4.9 %).

The biocompatibility of nanomedicines is important for the development of successful delivery systems. To examine the cytotoxicity of the blank and drug carrier nanoparticles HepG2 cells were treated with various concentration of nanoparticles. The active agent solution in DMSO was also investigated and all of the results were related to the negative control, that is, to the non-treated cells. As shown in Figure 8, cell viability remains around 90

% when exposed with 100 μg/well of both blank nanoparticles (50000 cells/well). The non-toxic feature of PEG-PLGA nanoparticles has already been verified by others (e.g. [4]). sorafenib showed a concentration dependent cytotoxicity in the HCC cells. The same concentration of free sorafenib exerted higher cytotoxicity compared to the microencapsulated sorafenib (Figure 11). Pure DMSO at equivalent volume of the free sorafenib solution in DMSO was also incubated with cells to evaluate its cytotoxicity effect that was found to be non-negligible. Accordingly, the cytotoxicity difference of free and entrapped sorafenib might have derived from the accompanying DMSO. Surprisingly, the highest sorafenib concentration changed the cell viability due to neither the free nor the encapsulated drug significantly.

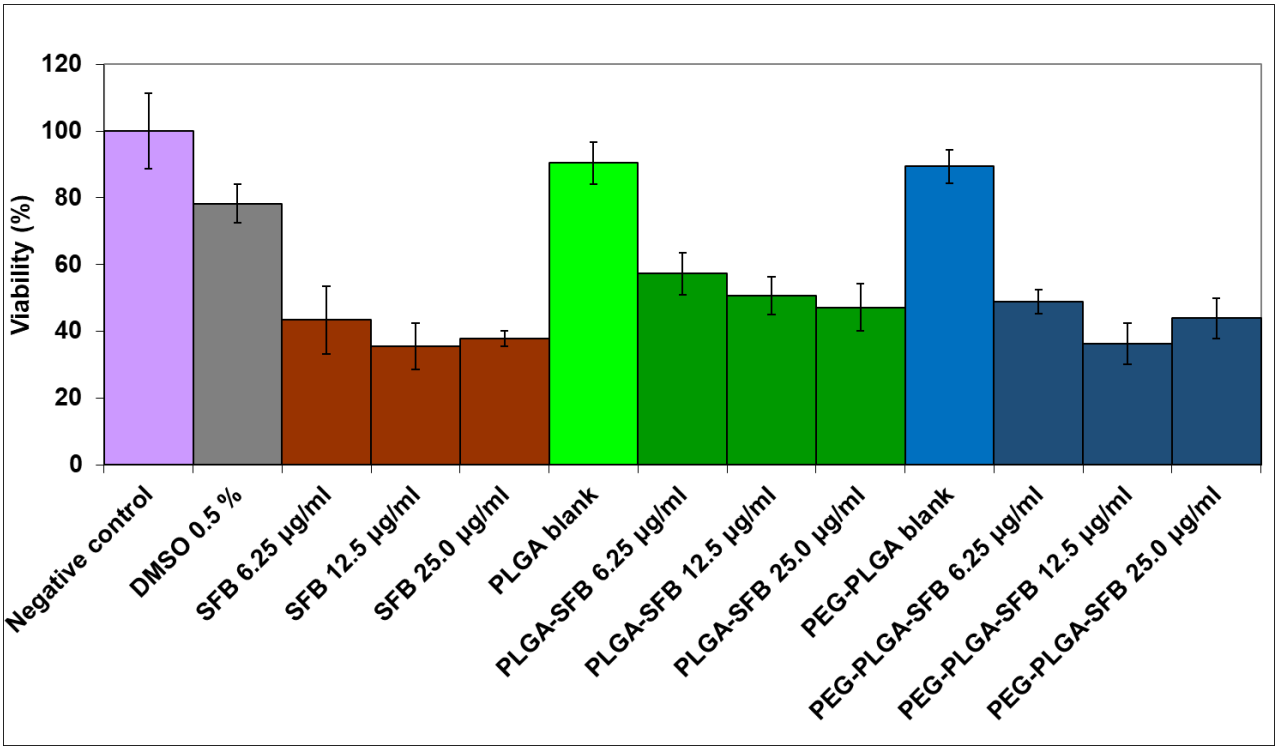

Figure 8: Viability of HepG2 cells treated with different concentrations of sorafenib, PLGA (RG 752H) or PEG-PLGA (RGP d 5055) nanoparticles and that of untreated cells (negative control).

5. Conclusions

Theranostic nanocomposites comprising PLGA or PEG-PLGA were loaded with the anti-cancer agent sorafenib and modified on their surface with the contrast agent Gd-DTPA. These

nanospheres exhibited superior properties compared to the particle systems described in the literature. Finally, the top-down manufacture combined with a modification of the particle surface using PEI and Gd-DTPA resulted in a strong MRI signal, optimal stability features and a sustained release profile. On this background further investigations will focus on the *in vivo* performance of these nanocarriers.

6. Experimental

a. Materials

Resomer® RG 502H (PLGA, lactide:glycolide: 50:50, inherent viscosity: 0.16-0.24 dl/g), Resomer® RG 752H (PLGA, lactide:glycolide: 75:25 inherent viscosity 0.14-0.22 dl/g), block copolymer Resomer® RGP d 5055 (PEG-PLGA, PEG content: 3-7 % (m/m), inherent viscosity: 0.93 dl/g) were obtained from Evonik Industries AG (Essen, Germany).

Polyvinyl alcohol (PVA, M_w=30,000-70,000, 87-90 % hydrolysed), Tween 80, Triton X-100, Pluronic F127 emulsifiers, dichloromethane (DCM), acetone, dimethyl sulfoxide (DMSO), sodium azide, D-trehalose dehydrate, mannitol, polyethyleneimine (MW 25 kDa), 1-ethyl-3(3-dimethylaminopropyl) carbodiimide (EDC), N-hydroxysuccinimide (NHS), diethylenetriaminepentaacetic acid gadolinium(III) dihydrogen salt hydrate (Gd-DTPA), HSA were obtained from Sigma Aldrich (St. Louis, MO). Sorafenib (free base) was purchased from LC Laboratories (Woburn, MA). Magnevist® was purchased from Bayer AG (Leverkusen, Germany). The mBCA (micro bicinchoninic acid) protein assay kit was bought at Pierce Biotechnology, Inc. (Waltham, MA).

b. Cell culture experiments in HepG2 cells

The human hepatoma cell line HepG2 was grown in Dulbecco′s modified Eagle′s medium supplemented with 10 % fetal calf serum, 100 U/ml penicillin and 100 µg/ml streptomycin.

The cells were cultured at 37 ºC in a humidified atmosphere containing 5 % CO2. The cells were trypsinized, resuspended and precultured before use.

c. Preparation of nanoparticles using nanoprecipitation

In brief, an amount of 5 to 10 mg of Resomer® RG 502 H, Resomer® RG 752H or Resomer® RGP d 5055 and 0.5 to 4 mg of sorafenib were dissolved in between 0.5 and 1.0 ml of acetone under magnetic stirring. A water phase with a volume of 2.0 to 4.0 ml was composed of an aqueous solution (0.5 to 2.0 % w/v) of emulsifying agent (Tween® 80, PMAA-Na, Triton X-100 or Pluronic® F127). Afterwards, the organic solvent was evaporated over a time period of 12 h at room temperature and 1 bar under constant stirring. The nanoparticles were centrifuged (Eppendorf 5424 R, Hamburg, Germany) at 20,000 rpm for 25 min, washed trice and redispersed in equal volume of MilliQ water.

d. Preparation of nanoparticles using the single emulsion technique

For the preparation of nanoparticles with the single emulsion-solvent evaporation method, the organic phase was prepared in two steps. An amount of 1 to 2 mg sorafenib was dissolved in 0.1 to 0.2 ml of acetone, and this solution was poured into a solution comprising 5 to 20 mg of Resomer® RG 502 H, Resomer® RG 752H or Resomer® RGP d 5055 in 1 to 2 ml DCM.
A volume of 4 to 8 ml of an aqueous solution of PVA (1 to 2 % w/v) was added and sonicated using a Sonoplus HD2070, MS73 probe (Bandelin, Berlin, Germany) at an amplitude of 10 % for 60 s. The organic solvent was evaporated over 2 h at atmospheric pressure and room temperature. The nanoparticles were washed as described above (see section 2.2.)

e. Preparation of nanoparticles using double emulsion-solvent evaporation technique

The double emulsion-solvent evaporation technique was tested for the co-encapsulation of HSA into the sorafenib nanoparticles. The entrapped protein was further used for the covalent modification of the particle surface using the Gd complex (see section 2.9.). In principle, the inner water phase was formed by 2.5 mg HSA in a volume of 0.1 ml of MilliQ water. This solution was added to the organic phase composed of 15 mg of Resomer® RG 752H or Resomer® RGP d5055 dissolved in 1.5 ml DCM combined with 1.5 mg of sorafenib dissolved in 0.15 ml acetone. The first emulsification was performed by sonication using a Sonoplus HD2070, MS73 probe (Bandelin, Berlin, Germany) at an amplitude 10 % for 30 s. Afterwards, the water-in-oil emulsion was pipetted into 6.0 mL of an aqueous solution of PVA (1 % (w/v)). The water-in-oil-in-water emulsion was formed by a second sonication step at an amplitude 15 % for 45 s. The organic solvents were evaporated over a time period of 2 h under magnetic stirring at atmospheric pressure and room temperature. The nanoparticles were centrifuged at 20,000 rpm for 25 min (Eppendorf Centrifuge 5424 R), washed trice and redispersed in 0.5 ml of phosphate buffer (pH 8), and after gravimetric analysis, the suspensions were diluted to 20 mg/ml nanoparticle concentration.

f. Particle morphology and particle size analysis

The morphology of nanocapsules was investigated after centrifugation and redispersion in the described medium. The samples were examined using a FEI Talos F200XG2 high-resolution analytical scanning/transmission electron microscope (S/TEM) operated at 200 keV (SEM, Thermo Fischer Scientific, Waltham, MA).

Additionally, the particle size and size distribution were determined using a Zetasizer Nano ZS (Malvern Instruments, Malvern, UK) equipped with a backscatter detector at an angle of 173°. The particles were characterized for the volume mean diameter and polydispersity index (PDI).

g. Storage stability of nanoparticle formulations

To improve the physical stability of the colloidal dispersion during the time of storage, the nanoparticles were freeze-dried, and their storage stability was investigated after 6 months of storage. A concentration of 3 % (w/v) of two lyoprotectors (trehalose dihydrate or mannitol) was evaluated. The solid concentration was adjusted to 7 mg/ml of nanoparticles and the samples were put into a Christ Epsilon 2–7 freeze dryer (Martin Christ GmbH, Osterode am Harz, Germany). The lyophilisation was conducted in two drying steps.

Initially, the temperature was decreased to −60 °C for 1 h to freeze the samples. Afterwards primary drying was initiated by evacuating the chamber to 0.94 mbar. In parallel, temperature was raised to −30 °C over a time period of 150 min. Then, the pressure was reduced to 0.006 mbar and the temperature was increased to −10 °C over a time period of 60 min. These conditions were maintained for 35 h. Second drying was accomplished at a temperature of 10 °C for 60 min and at 20 °C for 10 h. The freeze dried samples were stored at 4 °C for a total duration of 6 months and reconstituted in the same volume of MilliQ water. The nanocomposite size and size distribution after redispersion was characterized.

h. Nanoparticle yield and encapsulation efficiency

The nanoparticle yield was determined by microgravimetry. The drug loading and encapsulation efficiency were investigated dissolving an amount of 10 mg nanoparticles in 1 ml of DMSO. The solution was diluted to be within the detectable linear calibration range (1-20 μg/L). The absorbance of the solutions was measured spectrophotometrically (Hitachi U-3000, Tokyo Japan) at 285 nm.

i. Biorelevant in vitro drug release test using the centrifugation method

The biorelevant *in vitro* drug release test was conducted using a centrifugation method. In brief, an amount of 1.5 mg of the sorafenib-loaded nanocomposites was re-suspended in 1 ml of human blood plasma containing 0.03 % sodium azide as a preservative. The nanoparticle formulations in release medium were filled into 2 mL tubes, and incubated at a temperature of 37 °C in an Thermomixer (Eppendorf, Hamburg, Germany) for 12 days at 700 rpm. At predetermined time points, samples with a total volume of 0.2 ml were collected. After each sampling time point the medium was replenished. The nanoparticles were separated from the plasma by centrifugation (Eppendorf Centrifuge 5424 R, 20 min at 20,000 rpm). The pellet was dissolved in 0.5 ml DMSO and the sorafenib concentration was determined spectrophotometrically as described above.

j. Surface modification using human serum albumin and polyethyleneimine

The nanoparticle dispersions prepared by single emulsion technique were centrifuged and redispersed in phosphate buffer (pH 8) resulting in a nanoparticle concentration of 20 mg/ml. To increase the number of free amino groups on the particle surface, HSA or PEI were covalently bound to the nanoparticle surface. A 50-fold molar excess of EDC and the same excess of NHS, both calculated to the molar polymer concentration, were dissolved in 0.5 ml phosphate buffer (pH 8) and incubated for 60 min, centrifuged and washed three times, and redispersed in 1.5 ml phosphate buffer (pH 8).

The obtained carbodiimide-activated nanoparticle dispersion was given into 0.5 ml phosphate buffer (pH 8) solution containing equimolar amounts of HSA or PEI, and shaken overnight at 20°C in an Eppendorf Thermomixer (Hamburg, Germany) at 700 rpm. Afterwards, the nanoparticles were dialysed for 2 h against 400 ml of MilliQ water using a 100 kDa membrane to remove residues of the dissolved polymers HSA or PEI, respectively. The dialysis step was repeated with fresh MilliQ water.

k. Conjugation of nanoparticles using the Gd-DTPA complex

Gd complex was coupled to the HSA or PEI containing nanoparticles via the activation by the carbodiimide compound. In order to activate the carboxyl groups in the Gd complex a 10-fold molar excess of Gd-DTPA (related to the (PEG-)PLGA) was dissolved in 1 ml buffer (pH8) and combined with a 5-fold molar excess of EDC and a 5-fold molar excess of NHS related to the Gd-DTPA. The resulting solution was incubated for 50 min and added to the purified nanoparticle suspension overnight. Non-reacted Gd-DTPA, EDC and NHS were removed by dialysis using membrane 3.5 kDa against 500 ml MilliQ for 2 h, and after changing the dialysis medium with 500 ml fresh MilliQ, for another 2h. The dialysed nanoparticle suspension was centrifuged and redispersed in 1.5 ml phosphate buffer.

l. Quantification of human serum albumin using the mBCA method

The crosslinked or co-encapsulated HSA content of the nanocomposites was determined by the mBCA method after centrifuging 0.1 ml nanoparticle dispersion, and removing the supernatant, while the pellet was dissolved in 0.5 ml DMSO. This solution was diluted 10-fold with MilliQ water, and incubated for 1 h at 60 ºC with the same volume of freshly prepared mBCA reagents mixture. DMSO was added to the calibrating HSA solution with the same ratio. After cooling the coloured mixtures to room temperature for 20 min, their absorbance was evaluated by spectrophotometry at 562 nm (Hitachi U-3000, Tokyo, Japan).

m. Quantification of gadolinium using ICP-OES

The Gd concentration was measured using inductively coupled plasma optical emission spectroscopy using a Spectro Genesis ICP-OES (Germany) simultaneous spectrometer with axial plasma observation.

Multielemental standards (Merck, standard solutions for ICP) were used for calibration. The limits of detection of the element was calculated according to equation 2:

(2) $$Limit\ of\ detection = Background\ signal + 3 * SD_{Background} * f_{dilution}$$

The purified nanoparticles were dissolved in 5 M hydrochloric acid and diluted to be in the desired calibration range.

n. In vitro investigation of diagnostic features by magnetic resonance imaging

In vitro MRI was carried out using the box analysis to compare the contrast achieved with the nanoparticle suspension with that of Magnevist® (Gd-DTPA complex with meglumine) solution. A calibration was achieved by diluting Magnevist® to 0.01-2.5 mg/ml concentration. MR imaging was performed on 3.0-T scanner (Siemens Magnetom Trio, Siemens Medical Solutions, Erlangen, Germany). The measurement conditions were T1-weighted 3D gradient echo sequences (fast low-angle shot) with the following parameters: TE = 3.31 ms, TR = 8.67 ms, field of view = 100 x 78 mm, matrix acquisition = 640 x 480, slice thickness = 0.3 mm, flip angle = 16°, fat suppression = fat saturated, and bandwidth = 180 Hz/Px.

o. Labelling of nanoparticles with a fluorescent dye

A volume of 1.0 ml of the nanoparticle suspension (12 mg/ml) in phosphate buffer (pH 8) was mixed with 0.1 ml phosphate buffer (pH 8) involving 25x molar excess of EDC and NHS, related to the (PEG-)PLGA molar, and incubated for 60 min, centrifuged and washed, and redispersed in 1.0 ml phosphate buffer (pH 8). The obtained carbodiimide activated

nanoparticle dispersion was given to 0.1 ml PB (pH 8) solution containing 1 mg/ml Cyanine 5 amine fluorescent dye, and shaked 1 h at 20°C in an Eppendorf Thermomixer (Hamburg, Germany) at 700 rpm. Then, the nanoparticle dispersion was centrifuged by an Eppendorf Centrifuge 5424 R (Hamburg, Germany) with 20,000 rpm for 25 min, washed three times and redispersed in phosphate buffered saline to a nanoparticle concentration of 10 mg/ml.

p. *In* vitro cellular uptake and cytotoxicity

Cellular uptake of the nanoparticles into the HepG2 cells was evaluated using flow cytometry. The cells were cultured in 24-well plates at a cell density of $2x10^5$ cells per well at 37 °C and 5 % CO_2 for 24 h. After cultivation, 100 μg nanoparticles/well (10 mg nanoparticles/ml) was pipetted to the cells and incubated for 24 h. The cells grown without nanoparticles were used as control. The cells were washed by phosphate buffered saline (PBS), trypsinized and redispersed in PBS containing 2% BSA. Flow cytometry was performed on a Cytoflex S cytometer (Beckman Coulter, Brea, CA).

In vitro cytotoxicity caused in HepG2 cells was assayed using MTT reagent. Cells were seeded (50000 cells/well) in 96-well plates. After 24 h pre-incubation, the growth media were replaced with 100 μl of fresh DMEM containing 10 % FBS and PLGA-sorafenib or PEG-PLGA-sorafenib nanoparticles. Three different sorafenib concentration levels of the added nanoparticles were applied: 6.25 μg/ml, 12.5 μg/ml and 25 μg/ml, while the control samples were also supplied by the same concentration of free sorafenib in DMSO solution. After 24 h incubation 10 μl/well MTT solution (5 mg MTT/ml) was added followed by further incubation for 2 h. The supernatant was removed, and then 0.2 ml MTT lysis solution was added into each well. The absorbance of cell suspension was determined at 595 nm by a spectrophotometer (EnVision 2104 Multilabel Reader, Perkin Elmer, Waltham, MA). The percentage of viable cells was calculated by comparing the absorbance of treated cells against

the untreated cells (negative control). The data were presented as mean and standard deviation with 5 replicates.

q. Statistics

All data are expressed as the mean value ± standard deviation (SD), which were calculated and plotted using Microsoft Excel (Microsoft, Redmond, WA) and SigmaPlot 11.0 (Systat Software GmbH, Erkrath, Germany), respectively. All nanoparticle formulations were produced as three batches (n=3).

7. Abbreviations

DCM: dichloromethane

DMSO: dimethyl sulfoxide

EDC: 1-ethyl-3(3-dimethylaminopropyl) carbodiimide

Gd-DTPA: Diethylenetriaminepentaacetic acid gadolinium(III) dihydrogen salt hydrate

HCC: hepatocellular carcinoma

HSA: human serum albumin

mBCA: micro bicinchoninic acid

MRI: magnetic resonance imaging

NHS: N- hydroxysuccinimide

PB: phosphate buffer

PBS: phosphate buffered saline

PEI: polyethyleneimine

PLGA: poly(D,L-lactide-co-glycolide)

PLGA-PEG: polyethylene glycol-poly(D,L-lactide-co-glycolide)

PVA: polyvinyl alcohol

SEM: scanning electron microscope

8. Acknowledgements

The authors are grateful to the LOEWE initiative of the state of Hessen for financial support to the research center Translational Medicine and Pharmacology. Dr. Tivadar Feczkó acknowledges the funding of Alexander von Humboldt Foundation (Ref. No.: 3.3-UNG/1161203 STP and 3.3-1161203-HUN-HFST-E) and that of BIONANO_GINOP-2.3.2-15-2016-00017 project. S/TEM studies were performed at the electron microscopy laboratory of the University of Pannonia, established using grant no. GINOP-2.3.3-15-2016-0009 from the European Structural and Investments Funds and the Hungarian Government. This

research was also supported by the 1783-3/2018/FEKUSTRAT grant of the Hungarian Ministry of Human Capacities.

9. References

1. Torre, L. A.; Bray, F.; Siegel, R. L.; Ferlay, J.; Lortet-Tieulent, J.; Jemal, A. *CA Cancer J Clin* **2015**, *65* (2), 87-108.
2. Keating, G. M.; Santoro, A. *Drugs* **2009**, *69* (2), 223-40.
3. Heidarinasab, A.; Ahmad Panahi, H.; Faramarzi, M.; Farjadian, F. *Mater Sci Eng C Mater Biol Appl* **2016**, *67*, 42-50.
4. Li, Y. J.; Dong, M.; Kong, F. M.; Zhou, J. P. *Int J Pharm* **2015**, *489* (1-2), 83-90.
5. Watcharin, W.; Schmithals, C.; Pleli, T.; Koberle, V.; Korkusuz, H.; Huebner, F.; Zeuzem, S.; Korf, H. W.; Vogl, T. J.; Rittmeyer, C.; Terfort, A.; Piiper, A.; Gelperina, S.; Kreuter, J. *Eur J Pharm Biopharm* **2014**, *87* (1), 132-41.
6. Fahrlander, E.; Schelhaas, S.; Jacobs, A. H.; Langer, K. *Nanotechnology* **2015**, *26* (14), 145103.
7. Wacker, M.; Zensi, A.; Kufleitner, J.; Ruff, A.; Schutz, J.; Stockburger, T.; Marstaller, T.; Vogel, V. *Int J Pharm* **2011**, *414* (1-2), 225-32.
8. Villa Nova, M.; Janas, C.; Schmidt, M.; Ulshoefer, T.; Grafe, S.; Schiffmann, S.; de Bruin, N.; Wiehe, A.; Albrecht, V.; Parnham, M. J.; Luciano Bruschi, M.; Wacker, M. G. *Int J Pharm* **2015**, *491* (1-2), 250-60.
9. Mohamed, F.; van der Walle, C. F. *J Pharm Sci* **2008**, *97* (1), 71-87.
10. Von Hoff, D. D.; Mita, M. M.; Ramanathan, R. K.; Weiss, G. J.; Mita, A. C.; LoRusso, P. M.; Burris, H. A., 3rd; Hart, L. L.; Low, S. C.; Parsons, D. M.; Zale, S. E.; Summa, J. M.; Youssoufian, H.; Sachdev, J. C. *Clin Cancer Res* **2016**, *22* (13), 3157-63.
11. Wacker, M. G. Nanomedicines—A Scientific Toy or an Emerging Market? In *Polymer Nanoparticles for Nanomedicines: A Guide for their Design, Preparation and Development*; Vauthier, C.; Ponchel, G., Eds.; Springer International Publishing: Cham, 2016; pp 591-614.
12. Liu, J.; Boonkaew, B.; Arora, J.; Mandava, S. H.; Maddox, M. M.; Chava, S.; Callaghan, C.; He, J.; Dash, S.; John, V. T.; Lee, B. R. *J Pharm Sci* **2015**, *104* (3), 1187-96.
13. Kim, D. H.; Kim, M. D.; Choi, C. W.; Chung, C. W.; Ha, S. H.; Kim, C. H.; Shim, Y. H.; Jeong, Y. I.; Kang, D. H. *Nanoscale Res Lett* **2012**, *7* (1), 91.
14. Malarvizhi, G. L.; Retnakumari, A. P.; Nair, S.; Koyakutty, M. *Nanomedicine* **2014**, *10* (8), 1649-59.
15. Zhang, J.; Hu, J.; Chan, H. F.; Skibba, M.; Liang, G.; Chen, M. *Nanomedicine* **2016**, *12* (5), 1303-11.
16. Xiao, Y.; Liu, Y.; Yang, S.; Zhang, B.; Wang, T.; Jiang, D.; Zhang, J.; Yu, D.; Zhang, N. *Colloids Surf B Biointerfaces* **2016**, *141*, 83-92.
17. Maeda, H.; Wu, J.; Sawa, T.; Matsumura, Y.; Hori, K. *J Control Release* **2000**, *65* (1-2), 271-84.
18. Lin Ts, T.; Gao, D. Y.; Liu, Y. C.; Sung, Y. C.; Wan, D.; Liu, J. Y.; Chiang, T.; Wang, L.; Chen, Y. *J Control Release* **2016**, *221*, 62-70.
19. Riddick, T. M. *Control of colloid stability through zeta potential*; Livingston: Wynnewood, Pa., 1968.
20. Ratzinger, G.; Agrawal, P.; Korner, W.; Lonkai, J.; Sanders, H. M.; Terreno, E.; Wirth, M.; Strijkers, G. J.; Nicolay, K.; Gabor, F. *Biomaterials* **2010**, *31* (33), 8716-23.
21. Holzer, M.; Vogel, V.; Mantele, W.; Schwartz, D.; Haase, W.; Langer, K. *Eur J Pharm Biopharm* **2009**, *72* (2), 428-37.

22. Janas, C.; Mast, M. P.; Kirsamer, L.; Angioni, C.; Gao, F.; Mantele, W.; Dressman, J.; Wacker, M. G. *Eur J Pharm Biopharm* **2017**, *115*, 73-83.